Original Research Article

A comprehensive physicochemical, thermal, and spectroscopic characterization of zinc (II) chloride using X-ray diffraction, particle size distribution, differential scanning calorimetry, thermogravimetric analysis/differential thermogravimetric analysis, ultraviolet-visible, and Fourier transform-infrared spectroscopy

Mahendra Kumar Trivedi, Kalyan Kumar Sethi[1], Parthasarathi Panda[1], Snehasis Jana[1]

Trivedi Global Inc., Henderson, Nevada 89052, USA, [1]Trivedi Science Research Laboratory Pvt. Ltd., Bhopal, Madhya Pradesh, India

Abstract

Objective: Zinc chloride is an important inorganic compound used as a source of zinc and has other numerous industrial applications. Unfortunately, it lacks reliable and accurate physicochemical, thermal, and spectral characterization information altogether. Hence, the authors tried to explore in-depth characterization of zinc chloride using the modern analytical technique.

Materials and Methods: The analysis of zinc chloride was performed using powder X-ray diffraction (PXRD), particle size distribution, differential scanning calorimetry (DSC), thermogravimetric analysis/differential thermogravimetric analysis (TGA/DTG), ultraviolet-visible spectroscopy (UV-vis), and Fourier transform-infrared (FT-IR) analytical techniques.

Results: The PXRD patterns showed well-defined, narrow, sharp, and the significant peaks. The crystallite size was found in the range of 14.70–55.40 nm and showed average crystallite size of 41.34 nm. The average particle size was found to be of 1.123 (d_{10}), 3.025 (d_{50}), and 6.712 (d_{90}) μm and average surface area of 2.71 m^2/g. The span and relative span values were 5.849 μm and 1.93, respectively. The DSC thermogram showed a small endothermic inflation at 308.10°C with the latent heat (ΔH) of fusion 28.52 J/g. An exothermic reaction was observed at 449.32°C with the ΔH of decomposition 66.10 J/g. The TGA revealed two steps of the thermal degradation and lost 8.207 and 89.72% of weight in the first and second step of degradation, respectively. Similarly, the DTG analysis disclosed T_{max} at 508.21°C. The UV-vis spectrum showed absorbance maxima at 197.60 nm (λ_{max}), and FT-IR spectrum showed a peak at 511/cm might be due to the Zn–Cl stretching.

Conclusions: These in-depth, comprehensive data would be very much useful in all stages of nutraceuticals/pharmaceuticals formulation research and development and other industrial applications.

Keywords: Differential scanning calorimetry, particle size distribution, powder X-ray diffraction, thermogravimetric analysis, zinc chloride

Address for correspondence: Dr. Snehasis Jana, Trivedi Science Research Laboratory Pvt., Ltd., Bhopal - 462 026, Madhya Pradesh, India.
E-mail: jana@trivedisrl.com

Access this article online	
Quick Response Code:	Website: www.jpionline.org
	DOI: 10.4103/jphi.JPHI_2_17

How to cite this article: Trivedi MK, Sethi KK, Panda P, Jana S. A comprehensive physicochemical, thermal, and spectroscopic characterization of zinc (II) chloride using X-ray diffraction, particle size distribution, differential scanning calorimetry, thermogravimetric analysis/differential thermogravimetric analysis, ultraviolet-visible, and Fourier transform-infrared spectroscopy. Int J Pharma Investig 2017;7:33-40.

INTRODUCTION

Zinc (II) chloride ($ZnCl_2$) is a colorless or white chemical compound, which is hygroscopic in nature.[1] It is commonly used in nutraceutical and pharmaceutical industry as nutraceuticals, drugs, and diagnostic agents, i.e., a powerful astringent, mild antiseptic, mouthwash dentin desensitizer, and deodorant preparations.[2-4] Zinc chloride has the other applications includes protein precipitation, various insulin, and pharmaceutical preparations.[3-6] It is the source of supplement for zinc to the animal body helpful for recovery from the deficiency syndromes (i.e., parakeratosis, hypogeusia, anorexia, dysosmia, geophagia, hypogonadism, growth retardation, and hepatosplenomegaly) and maintains the healthy quality of life.[2,7] In human, zinc resides in almost all the body parts, organs, or tissues (i.e., muscle, retina, prostate, bone, skin, kidney, liver, pancreas, red blood cells, and white blood cells) and plays important roles in several biological processes.[8,9] It functions as a cofactor of various enzymes, including carbonic anhydrase, lactate dehydrogenase, alkaline phosphatase, and for both RNA and DNA polymerase.[7-9] It acts as a metallotherapeutic agent and possesses various pharmacological activities include fertility enhancing, anticancer, retinoprotective, and putative antiviral activities.[10,11]

Although zinc chloride is a very well-known compound and has numerous applications in the industries, i.e., nutraceuticals, pharmaceuticals, and chemicals.[2-6,12] Unfortunately, it scarce comprehensive, reliable, and accurate in-depth analytical information all together for the physicochemical, thermal, and spectroscopic characterization. However, to our knowledge, the structural characterization of zinc chloride using powder X-ray diffraction (PXRD), particle size distribution (PSD), differential scanning calorimetry (DSC), thermogravimetric analysis (TGA), differential thermogravimetric analysis (DTG), ultraviolet-visible spectroscopy (UV-vis) spectroscopy, and Fourier transform-infrared (FT-IR) spectrometry techniques have not yet been reported in details in any literature/book for the better understanding of its chemical structure. These analytical techniques provide specific characteristic information related to the physical, thermal, and structural characteristics information which are very useful in various fields of science and technology.[13,14] Therefore, the authors tried to explore and bring a new insight into the physicochemical, thermal, and spectroscopic characterization using PXRD, PSD, DSC, TGA/DTG, UV-vis, and FT-IR.

MATERIALS AND METHODS

Chemicals

$ZnCl_2$ was procured from TCI, Japan. All the other chemicals used in this experiment were analytical grade procured from local vendors.

Methods of analysis

The zinc chloride sample was evaluated using the various analytical techniques for its physicochemical and spectroscopic characterization.

Powder X-ray diffraction analysis

The XRD analysis was accomplished on PANalytical X'Pert Pro powder X-ray diffractometer system. The X-ray of wavelength (λ) 1.54056 Å was used. The data were collected in the form of a chart of the Bragg angle (2θ) versus intensity (counts/second), and a detailed table containing information on peak intensity counts, d-value (Å), relative intensity (%), and full-width half maximum (FWHM) (θ°) [Table 1]. From the XRD results, the crystallite size (G) was calculated using X'Pert data collector and X'Pert high score plus processing software. The crystallite size (G) was calculated from the Scherrer equation.[15,16] The method was based on the width of the diffraction patterns obtained in the X-ray reflected the crystalline region. The crystallite size (G) was calculated using the following Scherrer formula:

$$G = k\lambda/(b\text{Cos}\theta)$$

Where, k is the equipment constant (0.5), λ is the X-ray wavelength (0.154 nm), b in radians is the FWHM of the peak, and θ the corresponding Bragg angle.

The sample was prepared using 500.19 mg of zinc chloride. The sample holder ring was fixed to the sample preparation table, and the sample was prepared by back loading technique using the sample preparation kit. Then, it was spread with sufficient quantity in the holder ring to fill the ring cavity. The sample was pressed down using powder press block, and the surplus powder was scraped using a glass slide to get a densely packed specimen. The bottom plate was positioned onto the holder ring and clamp in position. The sample holder was removed from the sample preparation table by turning it upside down. A smooth surface of the sample was obtained to ensure the optimum results.[16]

Particle size distribution analysis

The average particle size and PSD were analyzed using Malvern Mastersizer 2000, UK, with a detection range

Table 1: Powder X-ray diffraction data with Bragg angle, *d*-spacing, relative intensities, areas, and crystallite size analysis of zinc (II) chloride

Bragg angle (°2θ)	*d*-spacing (Å)	Relative intensity (%)	FWHM (°2θ)	Area (°2θ)	Crystallite size (G, nm)
16.222	5.464	16.26	0.1004	22.66	44.29
17.205	5.154	32.53	0.1338	60.45	33.27
26.046	3.421	77.30	0.1338	143.64	33.77
29.957	2.983	91.95	0.1338	170.86	34.06
35.573	2.524	67.15	0.1338	124.78	34.56
38.866	2.317	74.97	0.1673	174.13	27.91
49.270	1.849	100.00	0.1338	185.81	36.21
49.813	1.831	48.53	0.1171	78.90	41.47
51.864	1.763	7.00	0.1004	9.75	48.78
52.877	1.732	13.60	0.2007	37.89	24.51
56.780	1.621	27.45	0.1171	44.63	42.76
57.974	1.591	20.14	0.1004	28.06	50.16
58.901	1.568	38.76	0.1004	54.01	50.39
62.325	1.490	17.89	0.1004	24.94	51.28
66.811	1.400	8.90	0.2676	33.08	19.72
72.682	1.301	45.24	0.1004	63.05	54.49
74.375	1.275	6.71	0.1004	9.34	55.10
75.163	1.264	5.20	0.1004	7.25	55.40
79.455	1.205	7.20	0.1224	16.53	46.83
83.341	1.150	1.93	0.4015	10.74	14.70
91.259	1.077	18.06	0.1224	41.48	51.54
92.427	1.067	20.80	0.1428	55.73	44.65
97.872	1.067	10.77	0.1224	24.74	54.89
Average				61.85	41.34

FMHM: Full width at half maximum

between 0.01 and 3000 μm. The sample was prepared with 0.15 g of zinc chloride added with 2 drops of span 85 and 10 mL of sunflower oil. The suspension was mixed with the mixer for 2 min. The sample unit was filled with the dispersant medium (sunflower oil) and operated the stirrer at 2500 rpm. Alignment of the optics was done and taken the background measurement. After the background measurement, the sample was added to the sample unit with constant monitoring the obscuration and stopped the addition of sample when the obscuration reached in between 15% and 20%. When the obscuration was stable, the measurement was taken six times. The histograms of the measurement were recorded. The particle size (μm) for at below 10% level (d_{10}), 50% level (d_{50}), and 90% level (d_{90}) were calculated from the histogram [Figure 1][17] and presented in Table 2. The calculations were done by the software Mastersizer 2000.

One common measure of the cumulative distribution is the span ($d_{90} - d_{10}$), and the relative span is a common calculation to quantify distribution width:[18]

$$\text{Relative span} = (d_{90} - d_{10})/d_{50}$$

Differential scanning calorimetry

The thermal properties of zinc chloride were analyzed using the DSC Q20 (TA Instruments, USA) differential scanning calorimeter. A volume of 8.9 mg of sample was weighed and sealed in aluminum pans and equilibrated at 25°C. Then, the sample was heated up to 600ºC at the heating rate of 10°C/min under nitrogen gas as purge atmosphere with a flow rate of 50 mL/min. The values of onset, endset, peak temperature, peak height (mJ or mW), peak area, and change in heat (J/g) for each peak were recorded.

Table 2: Particle size distribution (d_{10}, d_{50}, and d_{90}) and surface area analysis of the zinc (II) chloride

Measurement	d_{10} (μm)	d_{50} (μm)	d_{90} (μm)	Surface area (m^2/g)
1	1.120	3.022	6.968	2.72
2	1.123	3.027	6.976	2.71
3	1.122	3.023	6.970	2.71
4	1.123	3.022	6.969	2.71
5	1.127	3.029	6.977	2.71
6	1.123	3.025	6.972	2.71
Average	1.123	3.025	6.972	2.71

Thermogravimetric analysis/differential thermogravimetric analysis

The TGA was performed using instruments TGA Q50 (TA Instruments, USA) at a heating rate of 10ºC/min at the room temperature, i.e., 30°C to 900°C under a nitrogen atmosphere (sample mass 15.76 mg on a platinum pan). In TGA, the weight loss for each step was recorded in grams as well as the percent loss with respect to the initial weight along with the onset, endset, and peak temperature for each step was recorded. Similarly, in DTG, the onset, endset, peak temperature, and change in heat (J/g) of each peak were recorded.

Ultraviolet-visible spectroscopy analysis

The UV-vis spectroscopic analysis was carried out using Shimadzu UV-2450 (SHIMADZU, JAPAN) with UV Probe, Japan. The spectrum was recorded using 1 cm quartz cell that has a slit width of 1.0 nm. The wavelength ranges chosen for recording the spectrum was 190-800 nm. The absorbance spectra (in the range of 0.2–0.9) and absorbance maximum (λ_{max}) were recorded.

Fourier transform-infrared spectroscopy

FT-IR spectroscopy of zinc chloride was performed on Spectrum two (Perkin Elmer, USA) FT-IR spectrometer with the frequency array of 400–4000/cm using pressed KBr disk technique. The compound was run as pressed disks using 300.50 mg of KBr as the diluent and 1.87 mg of zinc chloride sample.

RESULTS AND DISCUSSION

Powder X-ray diffraction analysis

When an X-ray is incident on a crystal, it diffracts in a pattern according to the characteristic of the crystal structure. In PXRD, the diffraction pattern is obtained from the powder material, rather than an individual crystal and is often easier and more convenient than individual crystal diffraction. PXRD also obtains peak position (determined the *d*-spacing and lattice parameter of crystal structure), peak width, and peak intensity (determined by the contents of the unit cell) for the bulk material of a crystalline solid.[19]

The PXRD study was conducted to explore the crystalline pattern of zinc chloride. The diffractogram of zinc chloride represents the XRD patterns shown in Figure 2. The intensity data were collected in a Bragg's angle (2θ) range of 10–100° [Table 1]. The PXRD patterns showed well-defined, narrow, sharp, significant peak at 2θ position equal to 16.222°, 17.205°, 26.046°, 29.957°, 35.573°, 38.866°, 49.270°, 49.813°, 51.864°, 52.877°, 56.780°, 57.974°, 58.901°, 62.325°, 66.811°, 72.682°, 74.375°, 75.163°, 79.455°, 83.341°, 91.259°, 92.427°, and 97.872°. The presence of very sharp and intense peaks in the diffractograms of zinc chloride revealed that the sample was crystalline in nature. $ZnCl_2$ has four crystalline forms (polymorphs) such as α (tetragonal), β (tetragonal), γ (monoclinic), and δ (orthorhombic), and in each case, the Zn^{2+} ions are tetrahedrally coordinated to four chloride ions. The only stable form in the anhydrous stage is hexagonal (a = 0.6125, b = 0.6443, and c = 0.7693 nm) close-packed (δ) type.[20,21] These crystalline patterns represented the wurtzite crystal phase of $ZnCl_2$.

Diffraction occurs only when Bragg's Law ($n\lambda = 2d \sin\theta$) is the satisfied condition for constructive interference (X-rays 1 and 2) from planes with spacing *d* [Figure 3]. If beams diffracted by two different atom layers which are in phase, constructive interference occurs, and the diffraction pattern shows a peak [Figure 3].[22] The diffraction peaks converted to the *d*-spacing [Table 1] are 5.464, 5.154, 3.421, 2.983, 2.524, 2.317, 1.849, 1.831, 1.763, 1.732, 1.621, 1.591, 1.568, 1.490, 1.400, 1.301, 1.275, 1.264, 1.205, 1.150, 1.077, 1.067, and 1.067 Å, which allowed identification of zinc chloride because each mineral has a set of unique *d*-spacing. The *d*-spacing was in the range of 5.464–1.067 Å and decreased with increased 2θ values. Typically, this could be a set of standard *d*-spacing information to achieve the identification of the unknown samples.

The peak intensity (I) was reported as peak height intensity, that intensity was the above background [Table 1]. The relative intensity was recorded as the ratio of the peak intensity to that of the strongest peak (I_1) (relative intensity = $I/I_1 \times 100$). The integrated peak intensities also calculated by the area under the peak [Table 1]. The average peak area calculated for the zinc chloride was 61.85 (2θ). The relative intensities of the peaks could be altered due to texture (i.e., preferred crystallographic orientation) in the sample.[23]

The FWHM was the width of the diffraction peak (in radians) at a height half-way between the background and the peak maximum [Figure 3]. The FWHM is a very important parameter for the calculation of crystallite size. The individual crystallite size was calculated using the

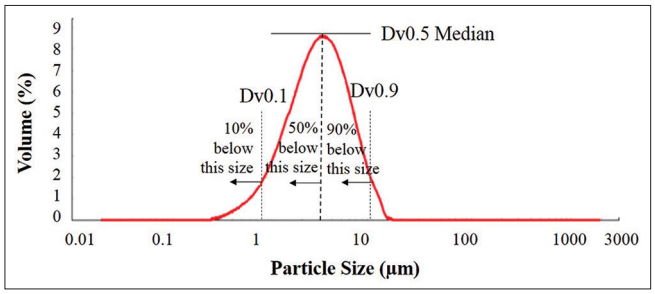

Figure 1: Particle size distribution (d^{10}, d^{50}, and d^{90}) histogram of zinc (II) chloride

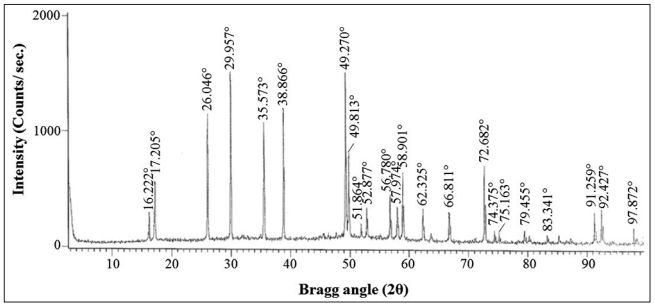

Figure 2: Powder X-ray diffraction patterns of zinc (II) chloride

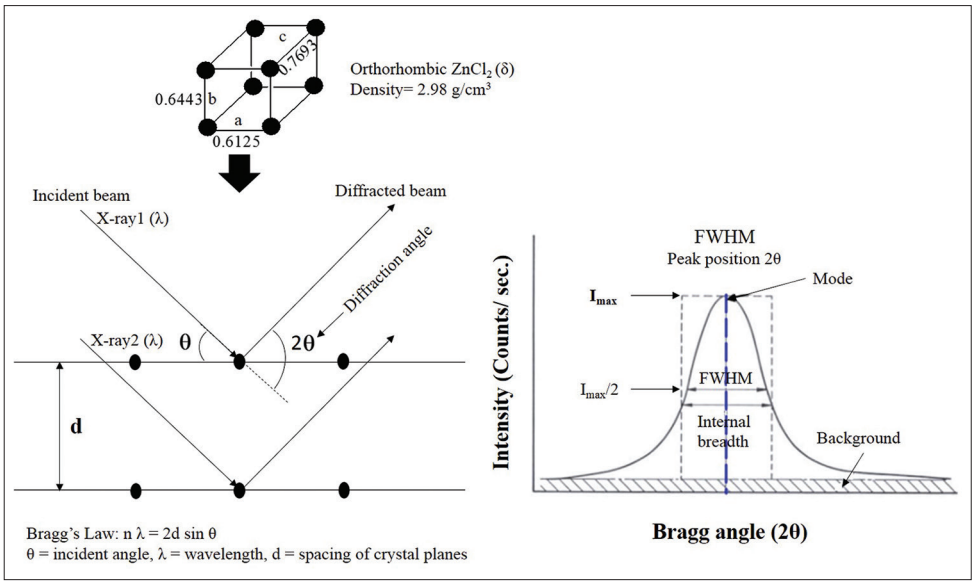

Figure 3: Powder X-ray diffraction peak profiles indicated that full-width at half-maximum of orthorhombic crystalline anhydrous zinc (II) chloride

Scherrer equation ($G = k\lambda/bCos\theta$).[15] The crystallite size was found to be in the range of 14.70–55.40 nm [Table 1]. The average crystallite size analysis of zinc chloride particles from the diffraction peak was found to be 41.34 nm. Increase in lattice strain may reduce the crystallite size of the sample.[24] The alternation in crystal morphology may cause the alteration in the relative intensities of the peaks.[16] The powder analysis information of zinc chloride by PXRD would be very much useful as a standard for future research in metallurgy, mineralogy, archeology, forensic science, condensed matter physics, and biological sciences. However, the PXRD analysis of $ZnCl_2$ is a rapid, nondestructive important technique in all stages of nutraceuticals and pharmaceuticals research and development.

Particle size distribution analysis

The particle size of zinc chloride was investigated, and the results are presented in Table 2. The common approach to define the distribution width was to cite three values on the X-axis, the d_{10}, d_{50}, and d_{90} diameter as shown in Figure 1. The 90% of the distribution lies below the d_{90}, and 10% of the population lies below the d_{10} diameter. Similarly, d_{50} diameter, the median, defined above the diameter where half of the population lies below this value. The experiment was repeated for six-time, and the average particle size and surface area were calculated The average particle size of the zinc chloride sample was 1.123 (d_{10}), 3.025 (d_{50}), and 6.712 μm (d_{90}) [Table 2]. Measurement of PSDs and understanding how they affect your products and processes can be critical to the achievement of many manufacturing industries. The PSD result indicated the average surface area of zinc chloride was 2.71 m^2/g. Surface area has a major influence on dissolution as a particle in a solvent. The reason that surface energy is the driving factor for dissolution efficiency and it is mainly influenced by surface area and chemical affinity. The span value was calculated to be 5.849 μm, and relative span value was 1.93 particularly for $ZnCl_2$. Rather than the use of these distribution points, it can be suggested to include other size parameters to describe the width of the distribution (i.e., span). The span is the distance between two points equally spaced from the median. The span is a common calculation to quantify cumulative distribution width. The significance of the span value describes relative dispersion, could be applied to all particle distributions, and deviations often under d_{10} and over d_{90}.[18]

The particle size and particle area have a significant impact on the performance and process handling of many particulate materials in nutraceuticals and pharmaceuticals.[25] The successful study of particle size analysis was rooted in an understanding of the distributions and the statistical terms describing zinc chloride.

Differential scanning calorimetry analysis

The thermal characterization of zinc chloride, i.e., fusion/decomposition temperature, and latent heat of fusion/decomposition were explored using DSC analysis and the results are presented in Figure 4 and Table 3. The DSC thermogram of zinc chloride represented the sharp exothermic peak. Thermal behavior of zinc chloride showed a small endothermic inflation at 308.10°C with the latent heat of fusion (ΔH) was about 28.52 J/g. The onset, peak, and endset temperature to the latent heat of

fusion were 297.96, 308.10, and 318.24°C, respectively. The enthalpy of melting (28.52 J/g) is the heat energy required for melting, i.e., for breaking down the zinc chloride crystalline lattice.[26] An exothermic reaction observed at about 449.32°C with the latent heat of decomposition (ΔH) was about 66.10 J/g. The onset, peak, and endset temperature to the latent heat of decomposition were 443.07, 449.32, and 452.86°C, respectively. The results indicated the decomposition is majorly dominated to that of fusion in the case of zinc chloride. The absence of glass transition temperature determines the crystal nature of zinc chloride.[26]

Thermogravimetric analysis/differential thermogravimetric analysis

The TG and DTG thermograms are shown in Figure 5a and b, respectively, for zinc chloride. In TGA, the method of thermal analysis in which changes in physical and chemical properties of materials were measured as a function of increasing temperature. The TG thermogram showed two steps of the thermal degradation process and the values were noted in Table 4. The pattern of thermal degradation of the zinc chloride was closely matched with one of the reported data.[27] The zinc chloride sample had lost 8.207 (1.294 mg) and 89.72% (14.14 mg) in the first and second step of degradation, respectively of their total original weight during this process [Figure 5a]. The major weight loss was in the second step of degradation (89.72%), which occurred in the temperature range of 309.30–564°C, which was complied with the DSC thermogram.

The DTG analysis exhibited two major peaks in the thermogram [Figure 5b] of zinc chloride. The thermogram of the sample disclosed maximum temperature (T_{max}) at 508.21°C. The onset, peak, and endset temperature to the T_{max} of maximum derivative weight loss was 357.36, 508.21, and 514.18°C, respectively. These TG/DTG thermal characteristic informations would be helpful for pharmaceuticals, nutraceuticals, and other industries handling zinc chloride.

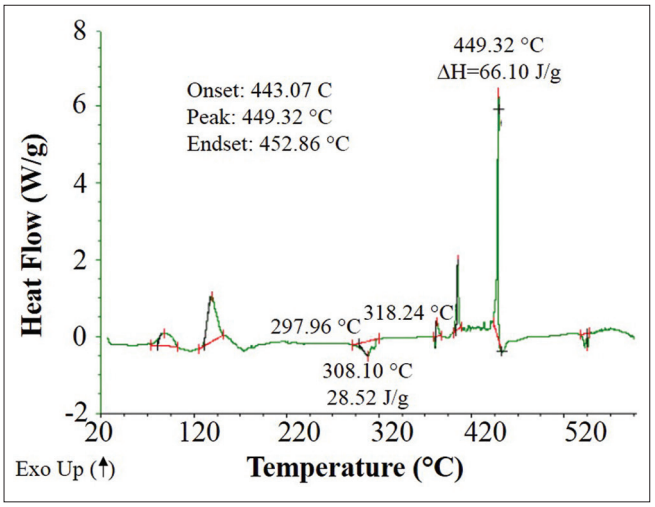

Figure 4: Differential scanning calorimetry thermogram of zinc (II) chloride

Ultraviolet-visible spectroscopy analysis

The UV-visible spectrum of zinc chloride is shown in Figure 6. The UV range of electromagnetic radiations is 180–400 nm, and the visible range is 400–800 nm. It was reported that the UV absorbance occurred due to excitation of electrons from the highest energy occupied molecular orbital to lowest energy unoccupied molecular orbital.[28] The UV spectrum of the zinc chloride sample exhibited the maximum absorbance at 197.6 nm (λ_{max}). The peak at 197.6 nm was indicated the absorbance maxima of 1.4992. The information of UV-visible characterization has not been reported elsewhere and would be helpful in analytical chemistry for the qualitative and quantitative analysis of the analyte in samples containing zinc chloride.

Fourier transform-infrared spectroscopy

The FT-IR spectrum of zinc chloride is presented in Figure 7. $ZnCl_2$ is a triatomic molecule that shows SP hybridization with a bond angle of 180°, which is linear in shape and may show four numbers of normal modes vibration ([3N-5 = 4] degrees of freedom; [n = 3]) at different regions of FT-IR spectrum [Figure 8].[29] The FT-IR spectrum showed the peak at 3586/cm (O-H stretching) in the spectrum [Figure 7] indicated the presence of -OH residues, which might be due to trapped moisture from the environment, while handling the sample for analysis. The usual nature of zinc chloride is hygroscopic and forms the hydrates of zinc chloride on exposure to water molecule ($ZnCl_2[H_2O]_n$; where n = 1, 1.5, 2.5, 3, and 4).[30] The H-O-H bending vibration at 1607/cm was observed in FT-IR spectrum [Figure 7] indicated the presence of water molecule(s). The metal halides (i.e., Zn–Cl) show IR peak in the range of 750–100/cm.[30] The peak found

Table 3: The latent heat (ΔH) of fusion/decomposition (J/g) and fusion/decomposition temperature (°C) of zinc (II) chloride

Parameter	ΔH (J/g)	Temperature (°C)		
		Onset	Peak	Endset
Latent heat of fusion	28.52	297.96	308.10	318.24
Latent heat of decomposition	66.10	443.07	449.32	452.86

Table 4: Thermal degradation data zinc (II) chloride

Steps of degradation	Temperature (°C)	Percentage weight loss (mg)
First step of degradation	27.34–309.30	8.207 (1.294)
Second step of degradation	309.30–896.10	89.72 (14.140)

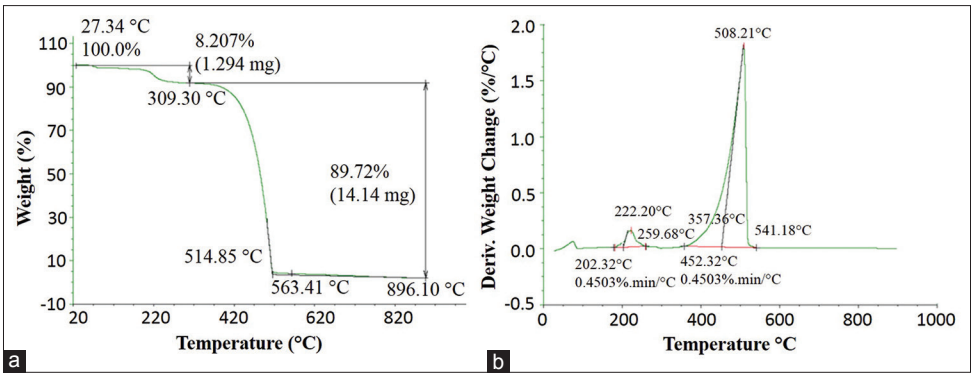

Figure 5: The (a) thermogravimetric analysis and (b) differential thermogravimetric analysis thermograms of zinc (II) chloride

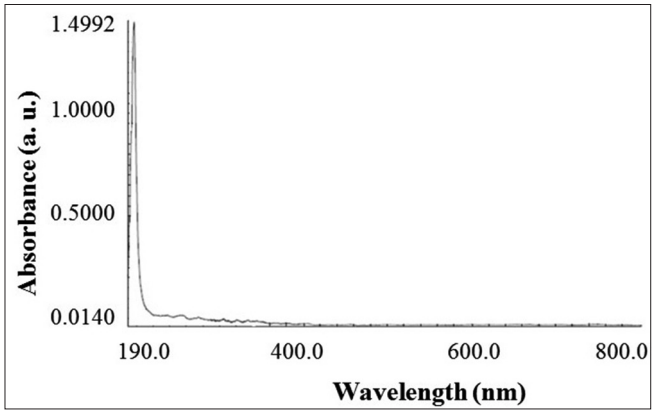

Figure 6: Ultraviolet-visible spectroscopy spectrum of zinc (II) chloride

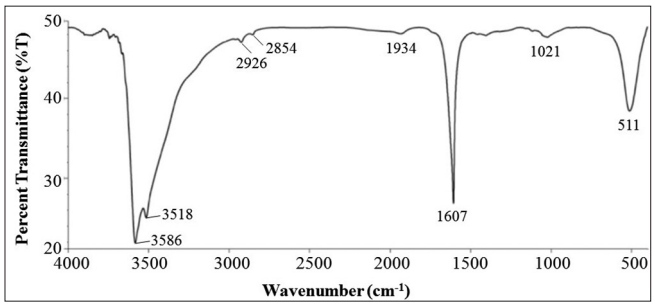

Figure 7: Fourier transform-infrared spectrum of zinc (II) chloride

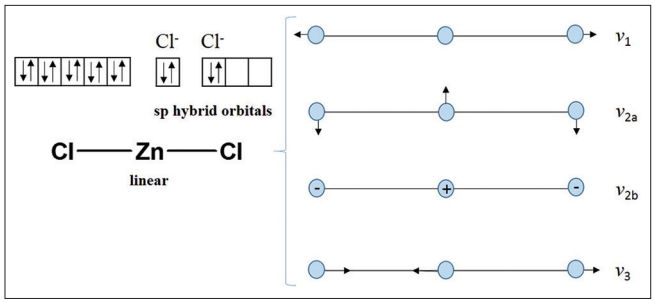

Figure 8: Hybridization and fundamental vibration of zinc (II) chloride

at 511/cm in the spectrum [Figure 7] could be due to the Zn–Cl stretching. The characteristic FT-IR spectroscopic information would be helpful to quick establishment of the presence or absence of the various vibrational modes of zinc chloride in various samples.

CONCLUSIONS

The current study effectively evaluated in-depth physicochemical, thermal, and spectroscopic characterization of $ZnCl_2$ using XRD, PSD, DSC, TG/DTG, UV-vis, and FT-IR. The zinc chloride PXRD patterns showed well-defined, narrow, sharp, significant peak at Bragg's angle (2θ) position, indicated the crystalline nature, and represented the wurtzite crystal phase. The *d*-spacing were found to be decreased with increased 2θ values. The average of peak area calculated for the zinc chloride was found to be 61.85 (2θ) and indicated average crystallite size of 41.34 nm. The PSD result indicated the average particle size of zinc chloride was 1.123 (d_{10}), 3.025 (d_{50}), and 6.712 μm (d_{90}) and average surface area of 2.71 m^2/g. The calculated span and relative span values were 5.849 μm and 1.93, respectively, particularly for zinc chloride. The DSC thermogram of zinc chloride showed a small endothermic inflation (ΔH fusion) and a larger exothermic peak (ΔH decomposition). The TGA thermogram showed two steps of the thermal degradation process and lost weight majorly in the second step of degradation during this process. Similarly, the DTG analysis exhibited two major peaks in the thermogram disclosed maximum temperature (T_{max}) at 508.21°C. The UV-visible spectrum showed absorbance maxima at λ_{max} of 197.6 nm. The FT-IR spectrum showed a peak at 511/cm was due to the Zn–Cl stretching. These comprehensive, physicochemical, and solid state characterization information of zinc chloride would be very useful assets and sets a standard for various fields of scientific research, qualitative and quantitative analysis, physical characterization of nutraceuticals, and pharmaceuticals having zinc chlorides as ingredients.

Financial support and sponsorship

The authors gratefully acknowledged to GVK Biosciences Pvt., Ltd., Hyderabad, India, for their support.

Conflicts of interest

There are no conflicts of interest.

REFERENCES

1. Brynestad J, Yakel HL. Preparation and structure of anhydrous zinc chloride. Inorg Chem 1978;17:1376-7.
2. Liu CH. Nutraceutical Combination for Prevention and Treatment of Type 2 Diabetes. U.S. patent US20160166631 A1; 2016.
3. Kasture AV, Wadodkar SG. A Text Book of Pharmaceutical Chemistry-1. Pune: Nirali Prakashan; 2008.
4. Mahadik KR, Kuchekar BS. Concise Inorganic Pharmaceutical Chemistry. Pune: Nirali Prakashan; 2008.
5. Raut NS, Deshmukh PR, Umekar MJ, Kotagale NR. Zinc cross-linked hydroxamated alginates for pulsed drug release. Int J Pharm Investig 2013;3:194-202.
6. Killedar SG, Nale AB, More HN, Nadaf SJ, Pawar AA, Tamboli US. Isolation, characterization, and evaluation of Cassia fistula Linn. seed and pulp polymer for pharmaceutical application. Int J Pharm Investig 2014;4:215-25.
7. Elmes ME. Letter: Zinc in human medicine. Lancet 1975;2:549.
8. Prasad AS. Clinical, biochemical, and pharmacological role of zinc. Annu Rev Pharmacol Toxicol 1979;19:393-426.
9. Supuran CT. Carbonic anhydrases: Novel therapeutic applications for inhibitors and activators. Nat Rev Drug Discov 2008;7:168-81.
10. Higdon JV, Ho E. Metallotherapeutic Drugs and Metal-Based Diagnostic Agents: The Use of Metals in Medicine. Weinheim: Wiley-VCH; 2005. p. 237.
11. McDaniel S, Goldman GD. Consequences of using escharotic agents as primary treatment for nonmelanoma skin cancer. Arch Dermatol 2002;138:1593-6.
12. Furniss BS, Hannaford AJ, Smith PW, Tatchell AR. Vogel's Textbook of Practical Organic Chemistry. 5th ed. New York: Longman/Wiley; 1989.
13. Mukharya A, Chaudhary S, Mansuri N, Misra AK. Solid-state characterization of lacidipine/PVP K(29/32) solid dispersion primed by solvent co-evaporation. Int J Pharm Investig 2012;2:90-6.
14. Kanthamneni N, Valiveti S, Patel M, Xia H, Tseng YC. Enhanced bioavailability of danazol nanosuspensions by wet milling and high-pressure homogenization. Int J Pharm Investig 2016;6:218-24.
15. Langford JI, Wilson AJ. Scherrer after sixty years: A survey and some new results in the determination of crystallite size. J Appl Crystallogr 1978;11:102-13.
16. Buhrke VE, Jenkins R, Smith DK. Preparation of specimens for X-ray fluorescence and X-ray diffraction analysis. New York: John Wiley & Sons; 1998. p. 148.
17. Burgess DJ, Duffy E, Etzler F, Hickey AJ. Particle size analysis: AAPS workshop report, cosponsored by the Food and Drug Administration and the United States Pharmacopeia. AAPS J 2004;6:e20.
18. Weiner BB. What is a continuous particle size distribution? New York, USA: Brookhaven Instruments; 2011.
19. Chauhan A, Chauhan P. Powder XRD technique and its applications in science and technology. J Anal Bioanal Tech 2014;5:212.
20. Mackenzie JD, Murphy WK. Structure of glass-forming halides. II. Liquid zinc chloride. J Chem Phys 1960;33:366-9.
21. Oswald HR, Jaggi H. On the structure of the anhydrous halides I. The anhydrous zinc chloride. Helv Chim Acta 1960;43:72-7.
22. Moore DM, Reynolds RC Jr. X-Ray Diffraction and the Identification and Analysis of Clay Minerals. 2nd ed. New York: Oxford University Press; 1997.
23. Sardela M. X-ray Analysis Methods. Advanced Materials Characterization Workshop, The Frederick Seitz Materials Research Laboratory-University of Illinois at Urbana-Champaign; 2008.
24. Balzar D, Audebrand D, Daymond MR, Fitch A, Hewat A, Langford JI, *et al*. Size-strain line-broadening analysis of the ceria round-robin sample. J Appl Crystallogr 2004;37:911-24.
25. Martin AN, Patrick JS. Martin's Physical Pharmacy and Pharmaceutical Sciences: Physical Chemical and Biopharmaceutical Principles in the Pharmaceutical Sciences. Philadelphia: Lippincott Williams & Wilkins; 2006.
26. Jones AT. Development of the γ-crystal form in random copolymers of propylene and their analysis by DSC and X-ray methods. Polymer 1971;12:487-508.
27. Martin FJ, Albers H, Lambeck PV, van de Velde GM, Popma TH. Luminescent thin films by the chemical aerosol deposition technology (CADT). J Aerosol Sci 1991;22:435-8.
28. Hesse M, Meier H, Zeeh B. Spectroscopic methods in organic chemistry. New York: Georg Thieme Verlag Stuttgart; 1997.
29. Wulfsberg G. Inorganic Chemistry. California: University Science Books; 2000.
30. Wiberg E, Wiberg N, Holleman AF. Inorganic Chemistry. San Diego: Academic Press; 2001.